RESEARCH REPORTS
Clinical

M. Kitamura[1], M. Akamatsu[2], M. Machigashira[3], Y. Hara[4],R. Sakagami[5], T. Hirofuji[6], T. Hamachi[7], K. Maeda[7], M. Yokota[8], J. Kido[9], T. Nagata[9], H. Kurihara[10], S. Takashiba[11], T. Sibutani[12], M. Fukuda[13], T. Noguchi[13], K. Yamazaki[14], H. Yoshie[14], K. Ioroi[15], T. Arai[16], T. Nakagawa[17], K. Ito[18], S. Oda[19], Y. Izumi[19], Y. Ogata[20], S. Yamada[21], H. Shimauchi[22], K. Kunimatsu[23], M. Kawanami[24], T. Fujii[25], Y. Furuichi[26], T. Furuuchi[27], T. Sasano[27], E. Imai[28], M. Omae[29], S. Yamada[1], M. Watanuki[2], and S. Murakami[30]*

[1]Department of Periodontology, Division of Oral Biology and Disease Control, Osaka University Dental Hospital; [2]Clinical Development Department, Kaken Pharmaceutical Co., Ltd.; [3]Department of Periodontology, Kagoshima University Dental Hospital; [4]Department of Periodontology, Nagasaki University Hospital, Attached School of Dentistry; [5]Section of Periodontology, Department of Odontology, Fukuoka Dental College Medical and Dental Hospital; [6]Section of General Dentistry, Department of General Dentistry, Fukuoka Dental College Medical and Dental Hospital; [7]Division of Oral Rehabilitation, Department of Periodontology, Kyushu University Hospital; [8]Division of Periodontology, Operative Dentistry and Endodontics, Department of Cariology and Periodontology, Kyushu Dental College Hospital; [9]Department of Periodontology and Endodontology, Tokushima University Hospital; [10]Division of Frontier Medical Science, Department of Periodontal Medicine, Hiroshima University Hospital; [11]Department of Pathophysiology - Periodontal Science, Biopathological Science, Okayama University Hospital; [12]Department of Periodontology, Division of Oral Infections and Health Science, Asahi University Dental Hospital; [13]Department of Periodontology, Aichigakuin University Dental Hospital; [14]Division of Periodontology, Department of Oral Biological Science, Niigata University Medical and Dental Hospital; [15]Department of Oral and Maxillofacial Surgery, Machida Municipal Hospital; [16]Department of Periodontics and Endodontics, Tsurumi University Dental Hospital; [17]Department of Dentistry and Oral Surgery, Keio University Hospital; [18]Department of Periodontology, Nihon University School of Dentistry Dental Hospital; [19]Section of Periodontology, Department of Hard Tissue Engineering, Tokyo Medical and Dental University, University Hospital, Faculty of Dentistry; [20]Department of Periodontology, Nihon University Dental Hospital at Matsudo; [21]Department of Periodontology, Tokyo Dental College Chiba Hospital; [22]Division of Periodontology and Endodontology, Department of Oral Biology, Tohoku University Hospital; [23]Division of Periodontology, Department of Conservative Dentistry and Oral Rehabilitation, Iwate Medical University Hospital, Dental Center; [24]Department of Periodontology and Endodontology, Division of Oral Health Science, Hokkaido University Hospital; [25]Department of General Dentistry, Health Sciences University of Hokkaido Hospital; [26]Division of Periodontology and Endodontology, Department of Oral Rehabilitation, Dental and Medical Clinic, Health Sciences University of Hokkaido; [27]Division of Oral Diagnosis, Department of Oral Medicine and Surgery, Tohoku University Graduate School of Dentistry; [28]Department of Nephrology, Nagoya University Graduate School of Medicine; [29]Department of Oral and Maxillofacial Surgery, Izumisano Municipal Hospital, Rinku General Medical Center; and [30]Department of Periodontology, Osaka University Graduate School of Dentistry, 1-8 Yamadaoka, Suita, Osaka 565-0871, Japan; *corresponding author, ipshinya@dent.osaka-u.ac.jp

J Dent Res 90(1):35-40, 2011

ABSTRACT

The efficacy of the local application of recombinant human fibroblast growth factor-2 (FGF-2) in periodontal regeneration has been investigated. In this study, a randomized, double-blind, placebo-controlled clinical trial was conducted in 253 adult patients with periodontitis. Modified Widman periodontal surgery was performed, during which 200 μL of the investigational formulation containing 0% (vehicle alone), 0.2%, 0.3%, or 0.4% FGF-2 was administered to 2- or 3-walled vertical bone defects. Each dose of FGF-2 showed significant superiority over vehicle alone ($p < 0.01$) for the percentage of bone fill at 36 wks after administration, and the percentage peaked in the 0.3% FGF-2 group. No significant differences among groups were observed in clinical attachment regained, scoring approximately 2 mm. No clinical safety problems, including an abnormal increase in alveolar bone or ankylosis, were identified. These results strongly suggest that topical application of FGF-2 can be efficacious in the regeneration of human periodontal tissue that has been destroyed by periodontitis.

KEY WORDS: periodontitis, tissue regeneration, fibroblast growth factor-2.

DOI: 10.1177/0022034510384616

Received April 19, 2010; Last revision June 29, 2010; Accepted July 3, 2010

A supplemental appendix to this article is published electronically only at http://jdr.sagepub.com/supplemental.

FGF-2 Stimulates Periodontal Regeneration: Results of a Multi-center Randomized Clinical Trial

INTRODUCTION

Periodontitis progressively destroys periodontal tissues and ultimately can lead to the loss of the affected teeth (Socransky and Haffajee, 2002; Ezzo and Cutler, 2003), and the ideal goal of periodontal treatment is complete regeneration of the tissues lost to periodontitis. Unfortunately, while conventional treatments, which mechanically remove the bacterial biofilm, show some success in suppressing the progression of periodontitis, they rarely actively induce periodontal regeneration. Thus, several surgical techniques, including bone grafting, guided tissue regeneration (GTR) treatment, and topical application of platelet-rich plasma or enamel matrix derivatives, have been developed in an attempt to accomplish this goal. Recently, the efficacy of recombinant human growth factors in periodontal regeneration is winning attention from researchers. Their biological properties have been extensively evaluated, and their consistent quality would be expected to reduce variations in regenerative responses.

Fibroblast growth factor (FGF)-2 exhibits potent angiogenic activity and mitogenic ability on mesenchymal cells within the periodontal ligament and has been reported to be effective in regenerating periodontal tissue in animal models (Takayama *et al.*, 2001; Murakami *et al.*, 2003; Kao *et al.*, 2009). Importantly, exploratory Phase 2A study showed that FGF-2 significantly improved the percentage of bone fill compared with vehicle alone, with about 2 mm CAL regained (Kitamura *et al.*, 2008).

The purpose of this study, the largest study in the field of periodontal regenerative therapy, was to clarify the efficacy and safety of FGF-2 and to determine the optimal dose for clinical use.

MATERIALS & METHODS

Study Design

A multi-center, randomized, double-blind, placebo-controlled, dose-finding study was conducted at 24 dental hospitals in Japan from September 2005 to March 2008.

This trial was conducted in accordance with the Good Clinical Practice Guidelines, and the protocol was reviewed and approved by the institutional review boards of each hospital.

Kaken Pharmaceutical Co., Ltd. (Tokyo, Japan) designed the study, and the academic authors participated in the development of the study design and protocol. Kaken also performed data gathering and analysis.

Eligibility of Patients

This study included male or female adult participants (age ≥ 20 yrs) with periodontitis, diagnosed as having 2- or 3-walled vertical periodontal tissue defects, 3 mm or deeper, apical to the remaining alveolar bone crest. In addition, patients' tooth mobility had to be Degree 2 or less, and the width of the attached gingivae had to be sufficient for GTR.

Patients were excluded if they had a malignant tumor or history thereof, severe diabetes (with a 6.5% or higher serum level of hemoglobin A1c), or hypersensitivity to protein drugs. Pregnant or nursing women were excluded. Patients with a consciousness disorder or severe disorders of the kidneys, liver, blood, or circulatory system were also excluded. All participants gave their written informed consent.

Randomization

Randomization was independently performed by the Registration Center (Adjust Co., Ltd., Sapporo, Japan). At each hospital, participants were randomly assigned to a block size of four, to receive 1 of 4 treatments: vehicle alone, 0.2% FGF-2, 0.3% FGF-2, or 0.4% FGF-2. Group assignment was not revealed until breaking of the blind.

Disallowed Medication and Procedures

The use of a calcium antagonist or adrenal cortical steroid (equivalent to 20 mg/day of Predonin) was disallowed within 4 wks after study drug administration. A surgical operation in the vicinity of the tooth selected for this study was disallowed within 36 wks after study drug administration.

Investigational Drug

This trial used recombinant human FGF-2 (Code No. KCB-1; Kaken Pharmaceutical Co., Ltd., Tokyo, Japan) produced by genetic recombination that transformed *Escherichia coli* with the human gene FGF-2. A gel-like investigational formulation was adopted for this study to improve drug administration to the region of alveolar bone defects. Before administration, the operators mixed freeze-dried FGF-2 with 3% hydroxypropyl cellulose, a colorless, viscous solution. The prepared investigational formulation (Code No. KCB-1D), containing 0% (vehicle alone), 0.2%, 0.3%, or 0.4% FGF-2, was administered within 24 hrs after preparation.

Study Intervention

All flap operations were performed in accordance with the modified Widman procedure, during which 200 μL of the investigational formulation were administered to the bone defect region. No specific root conditioning was performed. At 1, 2, and 4 wks after administration, the same clinical inspections were performed as before administration, and serum anti-FGF-2 antibodies were measured at 2 and 4 wks after administration. At 12, 24, and 36 wks following administration, standardized radiographs were taken, and periodontal tissues were inspected. In addition, ten patients from each group were randomly selected, and their serum FGF-2 levels were measured at 1, 2, 4, and 24 hrs after administration.

After breaking of the blind, at 72 wks after administration, a follow-up survey on bone fill, clinical attachment level (CAL), and adverse effects was conducted of all participant groups.

Outcome Measurements

The primary outcome was the percentage of bone fill shown by radiographs at 36 wks after administration. The geometrically standardized radiography used photograph indicators (Cone Indicator-II; Hanshin Technical Laboratory, Nishinomiya, Japan). Five doctors specializing in dental radiology at the Department of Oral Diagnosis at Tohoku University Graduate School of Dentistry (Sendai, Japan) independently measured the percentage of bone fill using methods described previously (Kitamura *et al.*, 2008). The median of the 5 measurements taken from the same image was then selected for efficacy analysis.

The secondary outcome was the CAL regained at 36 wks after administration. CAL, defined as the distance between the control point (the cement-enamel junction or margin of the restorative material) and the bottom of the gingival sulcus, was measured by investigators at each hospital. Prior to the initiation of baseline measurements, intra- and inter-examiner calibrations were performed on patients at each facility to ensure reproducibility and consistency by each investigator. All examiners used PCP-UNC-15 periodontal probes (Hu-Friedy, Chicago, IL, USA). Additionally, probing depth, bleeding on probing, gingival index, tooth mobility, gingival recession, plaque index, and width of keratinized gingivae were monitored during the study.

Sample Size Calculation

On the basis of the results from the exploratory study (Kitamura *et al.*, 2008), it was calculated that 49 participants were required for each group, assuming percentage bone fill of 24% in 'vehicle alone administered' participants and 58% in participants at either 0.2%, 0.3%, or 0.4% FGF-2 administration, a statistical power of 90%, and a two-sided type I error rate of 2.5% (for comparison of each FGF-2 group with the 'vehicle alone' group). Assuming that about ten participants in each group would be excluded due to discovery of bone defects non-conforming to inclusion criteria during flap operation, or due to withdrawal of consent, enrollment of 60 participants in each group was planned.

Statistical Analysis

SAS version 8.2 software (SAS Institute Inc., Cary, NC, USA) was used. For statistical comparison of the 3 dose groups in terms of efficacy endpoints with the 'vehicle alone' group, the Dunnett option was used, based on the Mixed procedure in the SAS system, in which adjusted p-values were computed for multiple comparisons, and analysis of the percentage of bone fill during follow-up was performed by repeated-measures analysis of variance with the Mixed procedure. Analysis was based on

the intention-to-treat (ITT) principle, with all participants included in their assigned groups.

RESULTS

Enrollment and Baseline Characteristics of the Participants

Patient flow through the study is shown in Fig. 1. Of 307 patients screened from August 2005 to April 2006, 267 patients were randomly assigned to one of the four groups. The characteristics at randomization are shown in Table 1. Fisher's exact probability test found no important imbalance regarding them.

Because 14 participants withdrew from the study before flap operation, 253 participants received the investigational drug. The safety and efficacy analyses were carried out on 253 and 249 participants, respectively.

Primary Outcome

All FGF-2 groups were significantly better than the 'vehicle alone' group ($p < 0.01$) for the primary outcome, the percentage of bone fill at 36 wks, in the ITT population (Table 2). Radiographs of a FGF-2-administered participant are shown in Fig. 2. Although all the groups showed improvement with time, significant differences were observed even at 12 wks in both the 0.3% and 0.4% FGF-2 groups (Table 2). Analysis of dose-response patterns by a maximum contrast method (Wakana *et al.*, 2007) showed that the percentage of bone fill at 36 wks reached a plateau in the 0.3% FGF-2 group.

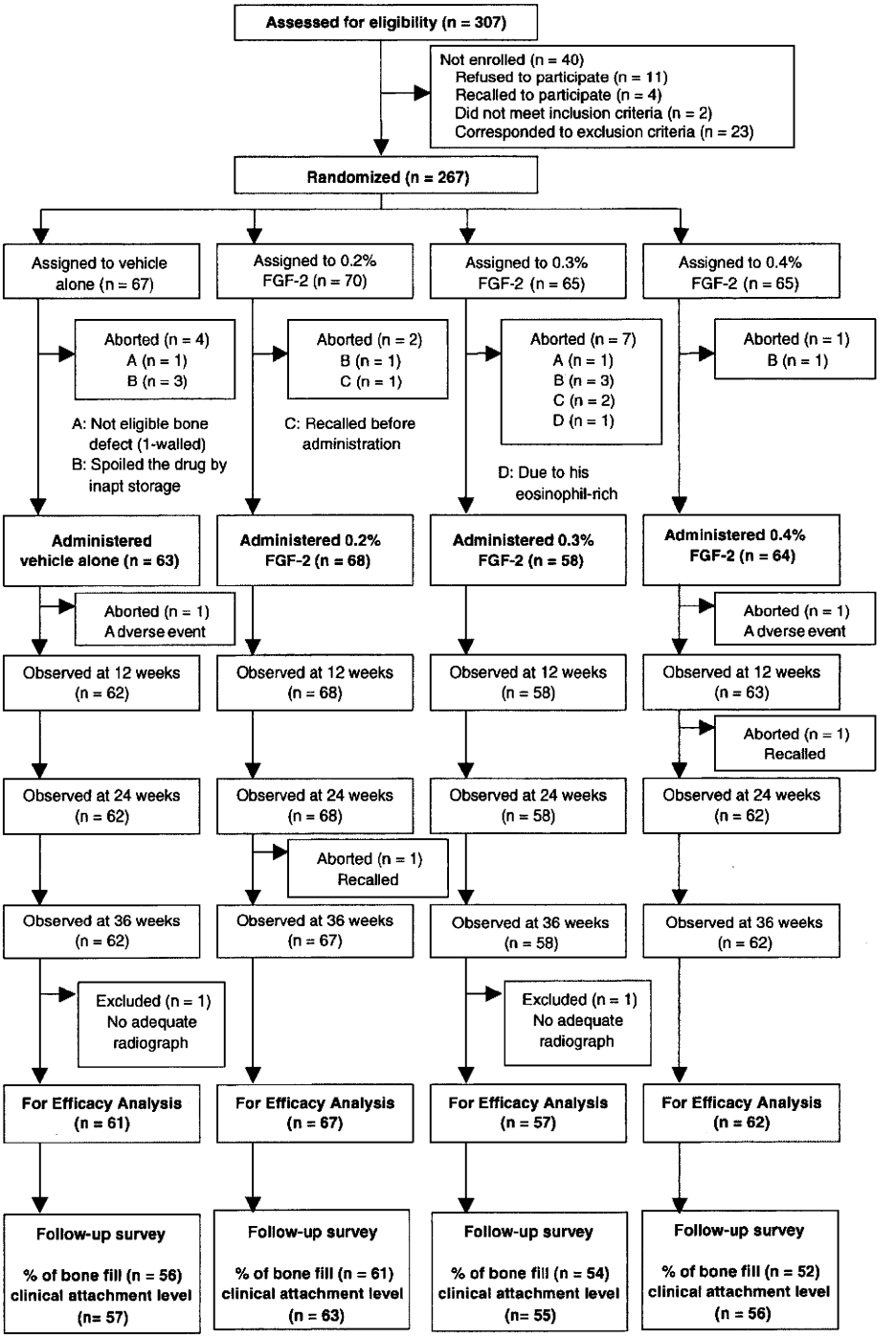

Figure 1. Patient flow diagram.

Secondary Outcome

The CAL regained after FGF-2 administration is shown in Table 2. No significant difference was observed among these 4 groups in the CAL regained, with all scoring around 2 mm.

Periodontal Inspections

Regarding probing depth, bleeding on probing, gingival index, tooth mobility, gingival recession, plaque index, and width of keratinized gingivae, no significant differences were observed among the 4 groups.

Safety

Adverse effects are listed in the Appendix Table. In addition, 10 participants from each of the groups were randomly selected, and blood samples were drawn. For 24 hrs after administration, the serum FGF-2 level was very low and

Table 1. Patient Characteristics

Item	Classification	Vehicle Alone	0.2% FGF-2	0.3% FGF-2	0.4% FGF-2
Numbers of patients		61	68	57	63
Sex (% of patients)	Male	42.6	47.1	36.8	50.8
	Female	57.4	52.9	63.2	49.2
Age (yrs)	Mean (SD)	52.2 (11.5)	53.2 (11.8)	52.8 (11.5)	52.5 (10.7)
Smoking habit (% of patients)	Yes	13.1	26.5	21.1	28.6
	No	86.9	73.5	78.9	71.4
Bone defect on x-rays (mm)	Mean (SD)	5.0 (1.8)	4.8 (1.6)	4.8 (1.7)	4.7 (1.6)
Probing depth (mm)	Mean (SD)	5.8 (1.6)	5.7 (1.5)	5.6 (1.4)	5.7 (1.4)
Width of keratinized gingiva (mm)	Mean (SD)	5.1 (2.3)	4.5 (2.2)	4.6 (2.1)	4.7 (1.9)
Bleeding on probing (% of patients)	–	26.2	33.8	24.6	34.9
	+	73.8	66.2	75.4	65.1
Gingival index (% of patients)	0	26.2	39.7	33.3	27.0
	1	34.4	23.5	28.1	41.3
	2	37.7	36.8	38.6	31.7
	3	1.6	0.0	0.0	0.0
Mobility (% of patients)	0	59.0	73.5	61.4	54.0
	1	37.7	20.6	26.3	39.7
	2	3.3	5.9	12.3	6.3
Plaque index (% of patients)	0	68.9	70.6	64.9	69.8
	1	29.5	27.9	33.3	28.6
	2	1.6	1.5	1.8	1.6

Each oral inspection was performed only at the test site around a participant tooth.

Table 2. Efficacy Endpoints

	Vehicle Alone			0.2% FGF-2				0.3% FGF-2				0.4% FGF-2			
	No. of patients	Mean	SD	No. of patients	Mean	SD	p value	No. of patients	Mean	SD	p value	No. of patients	Mean	SD	p value
% bone fill															
12 wks	59	4.65	13.93	67	6.44	17.08	0.925	57	15.89	23.96	0.009	63	13.34	24.18	0.049
24 wks	59	12.06	19.65	66	18.25	23.43	0.391	57	31.73	24.30	< 0.001	61	34.74	33.04	< 0.001
36 wks	61	15.11	21.90	67	33.24	33.15	0.003	57	50.58	31.46	< 0.001	61	46.56	36.09	< 0.001
72 wks*	56	15.86	22.14	61	39.11	37.32	< 0.001	54	52.15	38.12	< 0.001	52	48.85	34.14	< 0.001
CAL regained															
12 wks	61	1.59	1.52	67	1.81	1.51	0.758	57	1.85	1.26	0.670	63	1.79	1.72	0.795
24 wks	61	1.74	1.67	67	1.99	1.60	0.751	57	2.22	1.69	0.294	62	2.19	1.88	0.320
36 wks	61	1.79	1.51	67	2.12	1.74	0.555	57	2.32	1.68	0.224	62	2.23	1.89	0.349
72 wks*	57	2.12	1.72	63	2.48	1.79	0.572	55	2.35	1.78	0.850	56	2.46	1.91	0.636

*Data were obtained after breaking of the blind.

almost the same as before administration. Increased serum anti-FGF-2 antibodies were not observed in any participants after administration.

Follow-up Survey

Two hundred forty-six participants underwent the follow-up survey, since three individuals discontinued participation in the study (Fig. 1). Of these participants, none had an abnormal increase in alveolar bone exceeding the cement-enamel junction or an equivalent control point or ankylosis. The follow-up survey found that both bone fill and CAL regained at 72 wks were retained at the 36-wk level in all groups (Table 2).

DISCUSSION

The present study was designed as a Phase 2B study, with the purpose of clarifying efficacy and safety and to determine the optimal dose of FGF-2 for clinical use.

Regarding the percentage of bone fill at 36 wks, all FGF-2 groups were clearly superior to the 'vehicle alone' group. When the missing data were imputed by the last-observation-carried-forward method, the same results were produced (data not shown). A relative difference of 35% was observed between the 0.3% FGF-2 group and the 'vehicle alone' group in this primary outcome, which is in agreement with the assumed difference in the sample-size calculation. These results strongly

suggest that FGF-2 induced new alveolar bone formation at 36 wks.

The percentage of bone fill at 36 wks reached a plateau in the 0.3% FGF-2 group. In the 0.3% FGF-2 group, the percentage of bone fill began to increase at 12 wks after administration and continued to increase at the same rate up to 36 wks. However, a non-significant change (only 1.6%) in the percentage of bone fill was observed between 36 and 72 wks.

Several lines of evidence suggest that the following 2 mechanisms for the investigational drug enhanced periodontal tissue regeneration. First, FGF-2 directly stimulated proliferation of mesenchymal progenitor cells in the periodontal ligament while maintaining multi-lineage potential. The periodontal ligament has heterogeneous cell populations, and researchers have predicted the existence of some progenitor cells that can differentiate into cementoblasts or osteoblasts (Lekic *et al.*, 2001; Murakami *et al.*, 2003; Shimono *et al.*, 2003). Interestingly, a recent study reported that some cells within the ligament express STRO-1 and CD146 mesenchymal stem cell markers. Such cells, according to the study, differentiate into cementoblast-like cells, adipocytes, and collagen-forming cells. It is expected that FGF-2 induces clonal expansion of such cell populations. Second, FGF-2 stimulated angiogenesis and the production of various types of extracellular matrix, such as hyaluronan and osteopontin (Shimabukuro *et al.*, 2005; Terashima *et al.*, 2008), which plays a crucial role in creating the local environment desirable for periodontal tissue regeneration.

Approximately 2 mm of CAL had already been regained in all the groups at 12 wks after administration, when bone fill was only 15.89% improved, less than half of the improvement at 36 wks, even in the 0.3% FGF-2 group. However, no significant differences between groups were observed regarding CAL regained at 36 wks after administration. This non-significance was considered to be caused by the difference in healing patterns between the FGF-2 groups and the 'vehicle alone' group. Conventional periodontal surgery, which corresponds to the 'vehicle alone' group, usually causes long junctional epithelial attachments, while gingival epithelial cells migrate along the gingival connective tissue down to the root surface (Caton and Zander, 1976; Bowers *et al.*, 1982; Wikesjö and Nilvéus, 1991). This pattern of healing in the 'vehicle alone' group (epithelial attachment) does not require neogenesis of alveolar bone, cementum on the root surface, or fibrous attachment, but maintains resistance to probing force for a period of time. Because manual probing cannot precisely distinguish fibrous attachment from epithelial attachment, the difference in the pattern of healing cannot be reflected in CAL regained between the groups.

The safety analysis indicated that the frequency of adverse effects was not associated with group allocation (Fisher's exact test). Clinical examination showed that no FGF-2 entered the circulation, and that FGF-2 was not associated with antibody production. These results suggest little possibility that FGF-2 will cause systemic adverse effects after topical application. Although oral inspection revealed changing color of gingiva, gingival swelling, bleeding, and protracted gingival wound healing, the severity was slight, and all of these disappeared by 36 days after

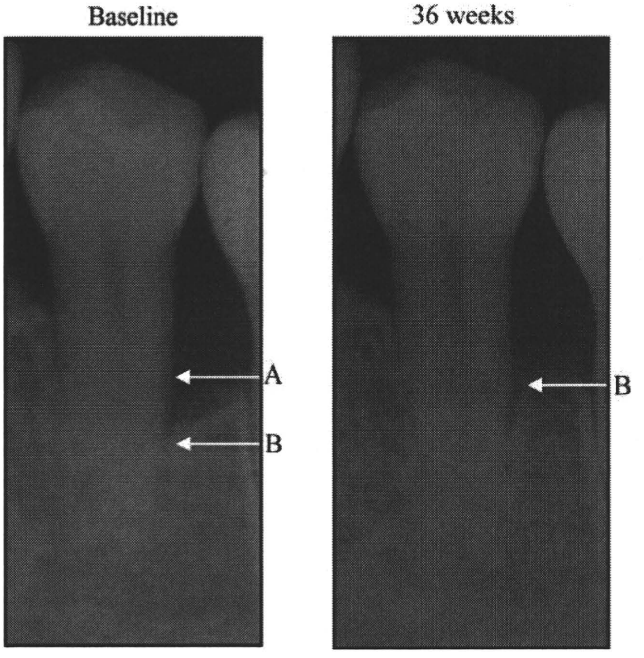

Figure 2. Radiographic outcome of a FGF-2-administered individual. A 0.3 % FGF-2-administered 39-year-old woman. The arrows indicate the remaining alveolar bone crest or the bottom of the bone defect. The depth of the intraosseous defect before administration was measured at 3.0 mm on the x-ray. The radiographs clearly show that the bone defect was filled with the newly generated alveolar bone at 36 wks after administration. The percentage of bone fill at 36 wks was 69.14%, with 3 mm CAL regained.

administration. In addition, no serious adverse effects were reported. Therefore, none of the present results suggests any clinical safety issues related to FGF-2 administration to patients.

Since the selection criteria were almost the same as those for general periodontal surgery, the efficacy results of this study are considered applicable to the general population of periodontitis patients. However, the occurrence of rare adverse effects cannot be completely addressed, because the scale of periodontitis patients in Japan is much larger than that in this study.

It has been reported that GTR treatment showed about 34% bone fill at 6 mos after surgery (Kilic *et al.*, 1997), and that enamel matrix derivatives (Zetterström *et al.*, 1997) and platelet-derived growth factor-BB plus beta-tricalcium phosphate (GEM-21S) (Nevins *et al.*, 2005) showed 31% and 57% bone fill, respectively, at 3 yrs and 6 mos after surgery. In this clinical trial, 0.3% FGF-2 achieved 50.6% bone fill at 9 mos. This suggests comparability with the current treatments in alveolar bone regeneration.

Thus far, histological observation has yet to be performed, due to ethical reasons. To overcome this limitation, we conducted a series of animal studies. These animal studies demonstrated that topical application of FGF-2 into artificially prepared intra-osseous defects in alveolar bones induced significant periodontal tissue regeneration. Furthermore, histological analyses revealed new cementum with Sharpey's fibers, new functionally oriented periodontal ligament fibers, and new alveolar bone (Takayama *et al.*, 2001; Murakami *et al.*,

2003; Kao *et al.*, 2009). These clinical and non-clinical studies suggest that topical application of FGF-2 is effective for the regeneration of human periodontal tissue that has been destroyed by periodontitis.

ACKNOWLEDGMENTS

We thank all the investigators and particularly all the participants for their important contributions to the study. S. Murakami received research grants from Kaken. M. Watanuki and M. Akamatsu are employees and stockholders of Kaken.

REFERENCES

Bowers GM, Schallhorn RG, Mellonig JT (1982). Histologic evaluation of new attachment in human intrabony defects. A literature review. *J Periodontol* 53:509-514.

Caton J, Zander HA (1976). Osseous repair of an infrabony pocket without new attachment of connective tissue. *J Clin Periodontol* 3:54-58.

Ezzo PJ, Cutler CW (2003). Microorganisms as risk indicators for periodontal disease. *Periodontol 2000* 32:24-35.

Kao RT, Murakami S, Beirne OR (2009). The use of biologic mediators and tissue engineering in dentistry. *Periodontol 2000* 50:127-153.

Kilic AR, Efeoglu E, Yilmaz S (1997). Guided tissue regeneration in conjunction with 10 hydroxyapatite-collagen grafts for intrabony defects. A clinical and radiological evaluation. *J Clin Periodontol* 24:372-383.

Kitamura M, Nakashima K, Kowashi Y, Fujii T, Shimauchi H, Sasano T, *et al.* (2008). Periodontal tissue regeneration using fibroblast growth factor-2: randomised controlled phase II clinical trial. *PLoS One* 3:e2611.

Lekic P, Rojas J, Birek C, Tenenbaum H, McCulloch CA (2001). Phenotypic comparison of periodontal ligament cells *in vivo* and *in vitro*. *J Periodontal Res* 36:71-79.

Murakami S, Takayama S, Kitamura M, Shimabukuro Y, Yanagi K, Ikezawa K, *et al.* (2003a). Recombinant human basic fibroblast growth factor (bFGF) stimulates periodontal regeneration in class II furcation defects created in beagle dogs. *J Periodontal Res* 38:97-103.

Murakami Y, Kojima T, Nagasawa T, Kobayashi H, Ishikawa I (2003b). Novel isolation of alkaline phosphatase-positive subpopulation from periodontal ligament fibroblasts. *J Periodontol* 74:780-786.

Nevins M, Giannobile WV, McGuire MK, Kao RT, Mellonig JT, Hinrichs JE, *et al.* (2005). Platelet-derived growth factor stimulates bone fill and rate of attachment level gain: results of a large multicenter randomised controlled trial. *J Periodontol* 76:2205-2215.

Shimabukuro Y, Ichikawa T, Takayama S, Yamada S, Takedachi M, Terakura M, *et al.* (2005). Fibroblast growth factor-2 regulates the synthesis of hyaluronan by human periodontal ligament cells. *J Cell Physiol* 203:557-563.

Shimono M, Ishikawa T, Ishikawa H, Matsuzaki H, Hashimoto S, Muramatsu T, *et al.* (2003). Regulatory mechanisms of periodontal regeneration. *Microsc Res Tech* 60:491-502.

Socransky SS, Haffajee AD (2002). Dental biofilms: difficult therapeutic targets. *Periodontol 2000* 28:12-55.

Takayama S, Murakami S, Shimabukuro Y, Kitamura M, Okada H (2001). Periodontal regeneration by FGF-2 (bFGF) in primate models. *J Dent Res* 80:2075-2079.

Terashima Y, Shimabukuro Y, Terashima H, Ozasa M, Terakura M, Ikezawa K, *et al.* (2008). Fibroblast growth factor-2 regulates expression of osteopontin in periodontal ligament cells. *J Cell Physiol* 216:640-650.

Wakana A, Yoshimura I, Hamada C (2007). A method for therapeutic dose selection in a phase II clinical trial using contrast statistics. *Stat Med* 26:498-511.

Wikesjö UM, Nilvéus R (1991). Periodontal repair in dogs. Healing patterns in large circumferential periodontal defects. *J Clin Periodontol* 18: 49-59.

Zetterström O, Andersson C, Eriksson L, Fredriksson A, Friskopp J, Heden G, *et al.* (1997). Clinical safety of enamel matrix derivative (EMDOGAIN) in the treatment of periodontal defects. *J Clin Periodontol* 24(9 Pt 2): 697-704.

Genes to Cells

Lectin microarray analysis of pluripotent and multipotent stem cells

Masashi Toyoda[1], Mayu Yamazaki-Inoue[1], Yoko Itakura[2], Atsushi Kuno[2], Tomohisa Ogawa[3], Masao Yamada[3], Hidenori Akutsu[1], Yuji Takahashi[1], Seiichi Kanzaki[1], Hisashi Narimatsu[2], Jun Hirabayashi[2] and Akihiro Umezawa[1]*

[1]*Department of Reproductive Biology, National Institute for Child Health and Development, 2-10-1 Okura, Setagaya-ku, Tokyo 157-8535, Japan*

[2]*Research Center for Medical Glycoscience, National Institute of Advanced Industrial Science and Technology, AIST Tsukuba Central 2, Tsukuba, Ibaraki 305-8568, Japan*

[3]*GP BioSceinces Ltd, 1-3-3, Azamino-Minami, Aoba-ku, Yokohama, Kanagawa 225-0012, Japan*

Stem cells have a capability to self-renew and differentiate into multiple types of cells; specific markers are available to identify particular stem cells for developmental biology research. In this study, we aimed to define the status of somatic stem cells and the pluripotency of human embryonic stem (hES) and induced pluripotent stem (iPS) cells using a novel molecular methodology, lectin microarray analysis. Our lectin microarray analysis successfully categorized murine somatic stem cells into the appropriate groups of differentiation potency. We then classified hES and iPS cells by the same approach. Undifferentiated hES cells were clearly distinguished from differentiated hES cells after embryoid formation. The pair-wise comparison means based on 'false discovery rate' revealed that three lectins -*Euonymus europaeus* lectin (EEL), *Maackia amurensis* lectin (MAL) and *Phaseolus vulgaris* leucoagglutinin [PHA(L)]- generated maximal values to define undifferentiated and differentiated hES cells. Furthermore, to define a pluripotent stem cell state, we generated a discriminant for the undifferentiated state with pluripotency. The discriminant function based on lectin reactivities was highly accurate for judgment of stem cell pluripotency. These results suggest that glycomic analysis of stem cells leads to a novel comprehensive approach for quality control in cell-based therapy and regenerative medicine.

Introduction

Stem cells produce almost every tissue of the human body. In general, they have the ability to divide and self-renew and to differentiate into various cell types. Stem cells have varying degrees of differentiation potential: (i) totipotency (ability to form the embryo and the trophoblast of the placenta) like fertilized eggs (zygotes); (ii) pluripotency (ability to differentiate into almost all cells that arise from the three germ layers) like human embryonic stem (hES) cells and induced pluripotent stem (iPS) cells; (iii) multipotentiality (capability of producing a limited range of differentiated cell lineages upon their location) like most tissue-based stem cells; and (iv) unipotentiality (ability to generate one cell type) like cells such as the epidermal stem cells and the spermatogonial cells of the testis. That is, a hierarchy of stem cells exists. In addition, human ES cell lines show variation in differentiation propensity (Osafune *et al.* 2008). iPS cells, another type of pluripotent stem cell, have been generated from somatic cells of different origin by retroviral transduction of four transcription factors (Takahashi *et al.* 2007; Yu *et al.* 2007). The established iPS cells have a wider variety of differentiation ability and gene expression when compared to ES cells (Aoi *et al.* 2008; Lee *et al.* 2009; Kaichi *et al.* 2010). However, a small proportion of these stem cells sometimes show spontaneous differentiation during serial passage. Therefore, to realize the potential for iPS cells to be utilized for cell therapy and as a valuable tool for drug discovery, it is necessary to monitor the status of these stem cells and to define

Communicated by: Takashi Tada
**Correspondence*: umezawa@1985.jukuin.keio.ac.jp

DOI: 10.1111/j.1365-2443.2010.01459.x

their exact stage during processes of growth and/or differentiation.

Glycosylation is a critical post- or co-translational modification found in more than 50% of eukaryotic proteins (Budnik *et al.* 2006). Thus, the glycome, which represents the total set of glycans expressed in a cell, is believed to be information-rich, as it varies among cell types, stages of development and differentiation, and even in the malignant transformation processes (Varki 1993). Lectins have long been used as tools to characterize cell surface glycans, such as for blood-group typing, tissue staining, lectin-probed blotting and flow cytometry (Sharon & Lis 2004). The use of lectins in glycan profiling provides considerable advantages. A modern technology to discriminate glycan profiling is lectin microarray analysis, which is an emerging technology that enables ultrasensitive detection of multiplex lectin–glycan interactions (Angeloni *et al.* 2005; Kuno *et al.* 2005; Pilobello *et al.* 2005). The system developed by Kuno *et al.* (2005) is based on a unique principle, that is, the evanescent-field fluorescence-detection principle, which has been used extensively for biosensors to study real-time binding events on the glass slide surfaces. Thus, the evanescent-field methods have greater advantage to analyze relatively weak interactions between lectins and glycoproteins in a liquid phase at equilibrium. Furthermore, this method is applicable for the analysis of the physiological and pathological status of crude glycoproteins extracted from mammalian cells (Ebe *et al.* 2006; Kuno *et al.* 2008) and cell surfaces (Tateno *et al.* 2007). Although the number of probes in lectin microarray is much smaller than in mRNA expression arrays, lectin microarray analysis enables high-throughput and sensitive analysis of a large set of biological samples and provides a snapshot of cell profiling. In this study, we further developed lectin microarray technology to define the status of somatic and pluripotent stem cells. The glycan-based comprehensive approach promises to be of great value, complementing more established methods such as gene expression analysis and epigenetic analysis.

Results

Lectin microarray analysis of mouse mesenchymal cells

Mesenchymal stem cells are multipotent and therefore may be useful in cell-based therapy along with ES cells and iPS cells. Mesenchymal stem cell (MSC) lines [(9-15c), osteoblasts (KUSA-A1), chondroblasts (KUM5) and preadipocytes (H-1/A)] were established from mouse bone marrow and were shown to retain potency both *in vivo* and *in vitro* (Umezawa *et al.* 1991; Matsumoto *et al.* 2005; Sugiki *et al.* 2007). To investigate their carbohydrate structures, we carried out a lectin microarray analysis of the cell membrane proteins. We quantified lectin signal using 'Array-Pro Analyzer' software and calculated the average net intensities of three spots for each lectin on the chip (Fig. 1A). Experiments with each cell line were performed in triplicate or quadruplicate. Four mesenchymal cell lines with different potencies showed differential lectin reactivities. 9-15c MSCs showed strong reactivity to wheat germ agglutinin (WGA), *Lycopersicon esculentum* lectin (LEL), concanavalin A (ConA), *Sambucus nigra* agglutinin (SNA) and *Ricinus communis* agglutinin I (RCA120) (Fig. 1A and Fig. S1 in Supporting Information). These signal intensities by lectin microarray were consistent with mean fluorescent intensities by flow cytometric analysis (Fig. 1B). We then performed hierarchical clustering analysis and principal component analysis (PCA) on the signal values of each lectin (Fig. 1C, D). H-1/A preadipocytes can be distinguished by KUM5 chondroblasts by lectin reactivities of GSL1A4, GSL1B4, BPL, PWM and MPA (PC1 axis), and 9-15c MSCs can be distinguished by KUSA-A1 osteoblasts by SNA. These cell types were reproducibly categorized into independent distinct groups.

Lectin microarray analysis of human mesenchymal cells

Human MSCs harvested from a variety of tissues have the capability to differentiate into numerous tissue lineages despite the fact that they may have tissue-specific characteristics. To clarify relationship between the tissue-specific characters of mesenchymal cells and glycomics, we performed lectin microarray analysis (LecChip™: Fig. S1 in Supporting Information) of mesenchymal cells derived from various tissues (Fig. 2A). Signal intensities by lectin microarray were consistent with the mean fluorescent intensities analysis determined by flow cytometric analysis (Fig. 2B). Hierarchical clustering analysis showed that human embryonic carcinoma NCR-G3 cells were reproducibly categorized into an independent group (red color in Fig. 2C), which is distinct from a group of mesenchymal cells derived from a variety of tissues (green color in Fig. 2C). In mesenchymal cells, bone marrow-, placenta- and extra finger-derived mesenchymal cells were categorized into distinct groups labeled in yellow, orange and blue, respectively (Fig. 2C).

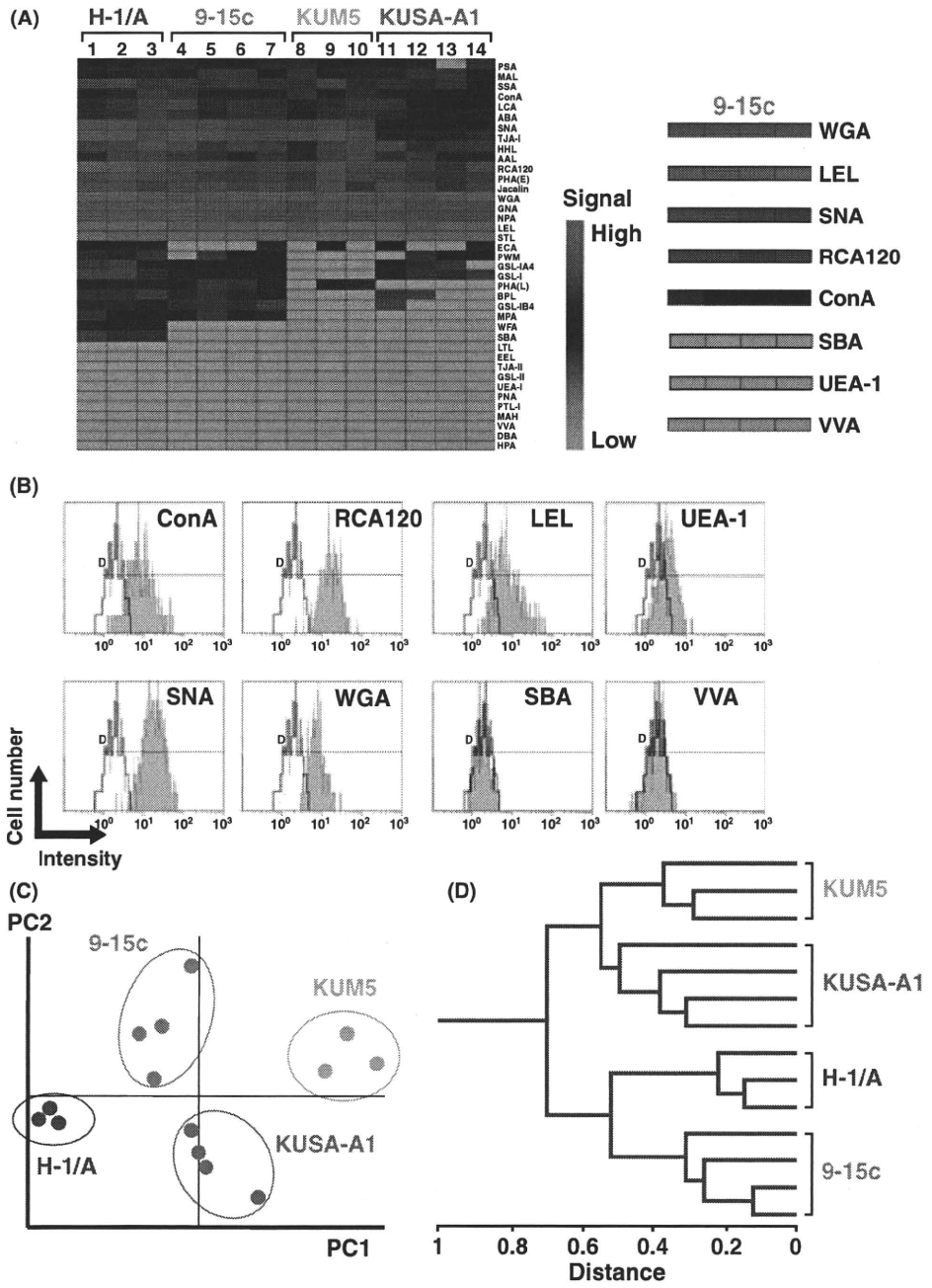

Figure 1 Lectin microarray analysis of mouse mesenchymal cells. (A) Heat map of 9-15c multipotent cells, KUSA-A1 osteoblasts, KUM5 chondroblasts and H-1/A preadipocytes. (B) Flow cytometric analysis of 9-15c multipotent cells using each lectin probe. Mean fluorescent intensities by flow cytometric analysis are consistent with signal intensities by lectin microarray. Nonshaded and shaded areas indicate reactivity of antibodies for isotype controls and that of antibodies for cell surface markers, respectively. (C) Principal component analysis of lectin microarray on mouse bone marrow–derived mesenchymal cells. Each cell is reproducibly subcategorized into groups of mesenchymal cell types. (D) Hierarchical clustering analysis of lectin microarray on mouse bone marrow–derived mesenchymal cells.

Human mesenchymal cells reacted to (i) *Pisum sativum* agglutinin (PSA), *Lens culinaris* agglutinin (LCA), *Aspergillus oryzae* lectin (AOL) and *Aleuria aurantia* lectin (AAL) that bind to Fucα1-6GlcNAc; (ii) SNA, *Sambucus sieboldiana* agglutinin (SSA) and *Trichosanthes japonica* agglutinin I (TJA-I) that bind to

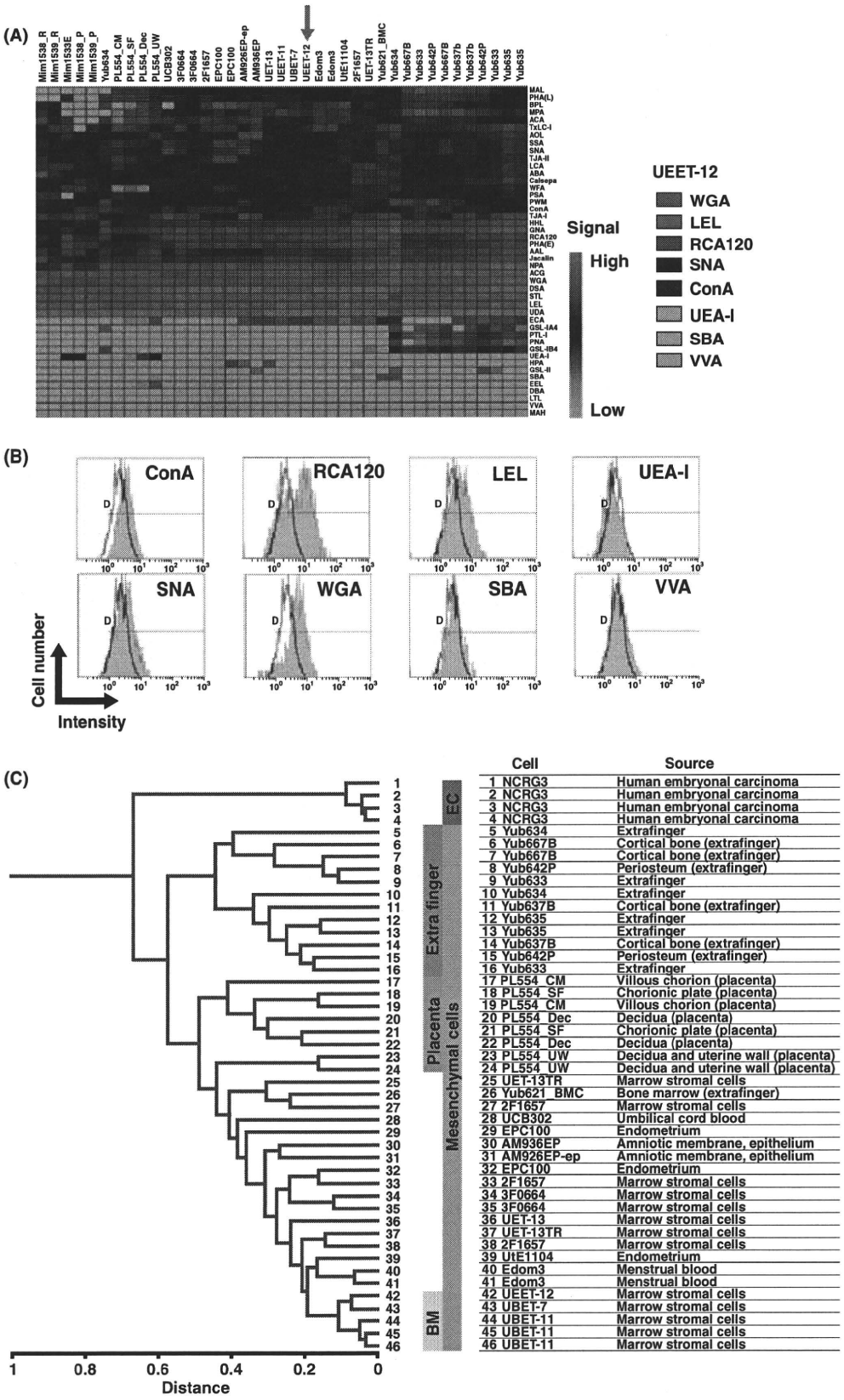

	Cell	Source
1	NCRG3	Human embryonal carcinoma
2	NCRG3	Human embryonal carcinoma
3	NCRG3	Human embryonal carcinoma
4	NCRG3	Human embryonal carcinoma
5	Yub634	Extrafinger
6	Yub667B	Cortical bone (extrafinger)
7	Yub667B	Cortical bone (extrafinger)
8	Yub642P	Periosteum (extrafinger)
9	Yub633	Extrafinger
10	Yub634	Extrafinger
11	Yub637B	Cortical bone (extrafinger)
12	Yub635	Extrafinger
13	Yub635	Extrafinger
14	Yub637B	Cortical bone (extrafinger)
15	Yub642P	Periosteum (extrafinger)
16	Yub633	Extrafinger
17	PL554_CM	Villous chorion (placenta)
18	PL554_SF	Chorionic plate (placenta)
19	PL554_CM	Villous chorion (placenta)
20	PL554_Dec	Decidua (placenta)
21	PL554_SF	Chorionic plate (placenta)
22	PL554_Dec	Decidua (placenta)
23	PL554_UW	Decidua and uterine wall (placenta)
24	PL554_UW	Decidua and uterine wall (placenta)
25	UET-13TR	Marrow stromal cells
26	Yub621_BMC	Bone marrow (extrafinger)
27	2F1657	Marrow stromal cells
28	UCB302	Umbilical cord blood
29	EPC100	Endometrium
30	AM936EP	Amniotic membrane, epithelium
31	AM926EP-ep	Amniotic membrane, epithelium
32	EPC100	Endometrium
33	2F1657	Marrow stromal cells
34	3F0664	Marrow stromal cells
35	3F0664	Marrow stromal cells
36	UET-13	Marrow stromal cells
37	UET-13TR	Marrow stromal cells
38	2F1657	Marrow stromal cells
39	UtE1104	Endometrium
40	Edom3	Menstrual blood
41	Edom3	Menstrual blood
42	UEET-12	Marrow stromal cells
43	UBET-7	Marrow stromal cells
44	UBET-11	Marrow stromal cells
45	UBET-11	Marrow stromal cells
46	UBET-11	Marrow stromal cells

Figure 2 Lectin microarray analysis of human mesenchymal cells. (A) Heat map on human cells derived from extra finger (auricular cartilage), bone marrow, umbilical cord blood, amnion, menstrual blood and endometrium. (B) Flow cytometric analysis of UEET-12 marrow stromal cells using each lectin probe. Nonshaded and shaded areas indicate reactivity of antibodies for isotype controls and that of antibodies for cell surface markers, respectively. (C) Hierarchical clustering analysis was performed based on the results of lectin microarrays. Human embryonic carcinoma cells (NCR-G3) and mesenchymal cells are discriminated by color bars (EC: red, mesenchymal cells: green, bone marrow (BM): yellow, placenta: orange, extra finger: blue).

Siaα2-6Gal/GalNAc; (iii) *Narcissus pseudonarcissus* agglutinin (NPA), ConA, *Galanthus nivalis* agglutinin (GNA) and *Hippeastrum hybrid* lectin (HHL), that bind to high-mannose structures; (iv) *Datura stramonium* agglutinin (DSA), LEL, *Solanum tuberosum* lectin (STL), *Urtica dioica* agglutinin (UDA), Pokeweed mitogen (PWM) and WGA that bind to GlcNAcβ1-4GlcNAc. Osteoblasts specifically reacted to *Griffonia simplicifolia* lectin I, isolectin (GSL I) A4 and its isolectin B4 that bind to α-GalNAc and α-Gal, respectively, Peanut agglutinin (PNA) that binds to Galβ1-3GalNAc and *Psophocarpus tetragonolobus* lectin I (PTL I) that binds to α-GalNAc (Fig. S1 in Supporting Information). These results suggested the lectin microarrays are a practical tool for glycan-based category of human mesenchymal cells, and that each cell type in the various cell lineages have specific carbohydrate structures.

Lectin microarray analysis of hES cells

To study glycans during differentiation of hES cells, we performed lectin microarray analysis with extracts from undifferentiated hES cells (hES-3, 8, 9 provided from Harvard University) and differentiated hES cells after embryoid body formation (EB) (Fig. S2 in supporting Information). The lectin microarray data after statistical analysis show that undifferentiated hES cells and differentiated cells (EB) were clearly categorized (Fig. 3A). To select lectins to discriminate between ES (pluripotent) and EB (nonpluripotent) cells, we analyzed lectin signals using 'pair-wise comparison means' based on FDR (False Discovery Rate) statistics. Three lectins [MAL, PHA(L) and EEL that bind to Siaα2-3Galβ1-4GlcNAc, tri/tetra-antennary complex-type N-glycan and Galα1-3Gal, respectively] could discriminate between the individual cell populations (FDR <0.05, fold-change >2.0) (Fig. 3B). The signals of MAL and PHA(L) in hES population were lower than those in EB, whereas the EEL signal in ES was higher than that in EB (Fig. 3C, D).

Lectin microarray analysis of iPS cells

We generated human iPS cell lines from MRC-5 embryonic lung fibroblasts (Makino *et al.* 2009) (Table S4 in Supporting Information) and performed

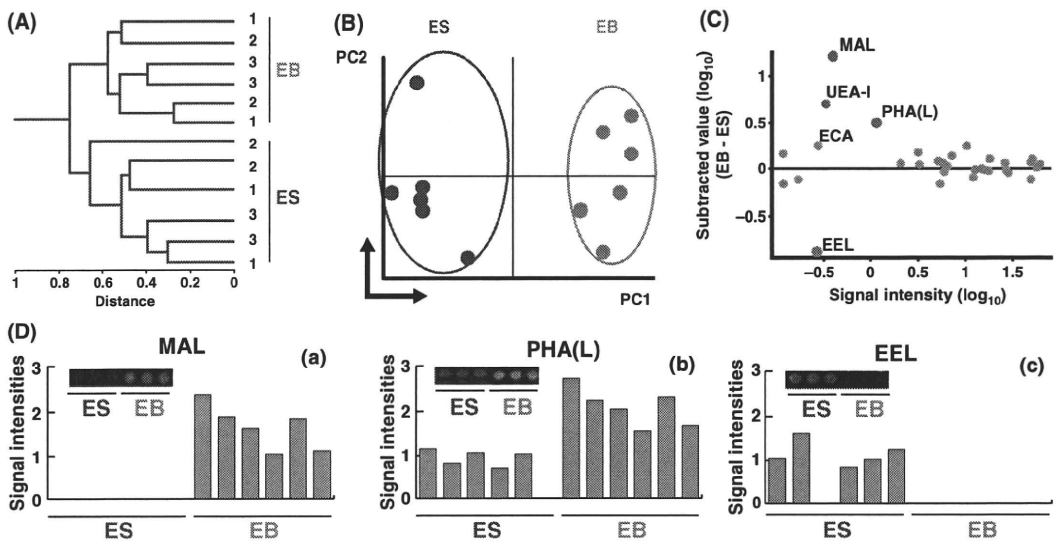

Figure 3 Lectin microarray analysis of human embryonic stem cells. (A) Hierarchical Clustering analysis of undifferentiated and differentiated ES cells. (B) Principal component analysis of lectin microarray analysis on undifferentiated and differentiated ES cells. (C) Signal value for *Maackia amurensis* lectin (MAL) processed by a max-normalization procedure after a gain-merging process. (D) Images of signal spots and signal intensities for MAL (a), PHA(L) (b), and *Euonymus europaeus* lectin (EEL) (c).

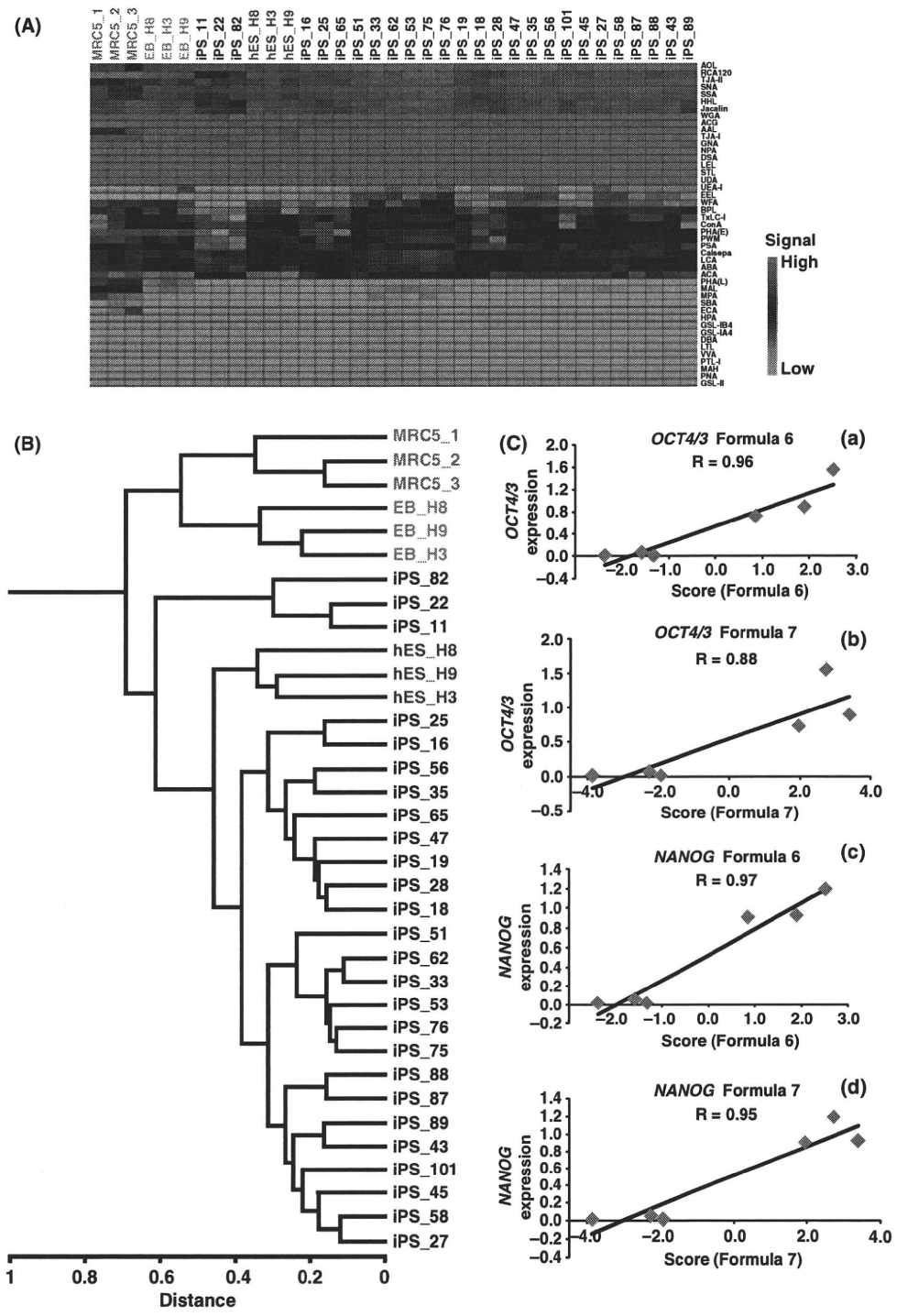

Figure 4 Lectin microarray analysis of human-induced pluripotent stem (iPS) cells. (A) Heat map of lectin microarray with MRC-5 and MRC-5-derived iPS cells. MRC-5 and iPS cells are discriminated by letter color: red, MRC-5; blue, hES cells; green, embryoid body (EB) cells; black, iPS cells. (B) Hierarchical Clustering analysis of MRC-5 and MRC-derived iPS cells. MRC-5 and iPS cells are discriminated by letter color: red, MRC-5; blue, hES cells; green, EB cells; black, iPS cells. (C) The correlation between expression of *OCT4/3* or *NANOG* and scores calculated from each formula. The correlation factors (R) are shown in each panel.

lectin microarray analysis of these cells and their parental MRC-5 cells. The iPS cell lines were clearly distinguishable from their parental cell MRC-5 (Fig. 4A,B). We then performed the lectin microarray analysis on iPS lines and their differentiated forms. All differentiated ES cells (EB; EB_H8, EB_H9 and EB_H3) were categorized into the group including MRC-5 parental cells, and undifferentiated iPS cells were categorized into the same group with hES cells (Fig. 4B). These results suggest that glycomic analysis using lectin microarray presents a specific lectin profile for pluripotency.

Generation of discriminant functions for pluripotency of human stem cells

To define pluripotency of human ES and iPS cells, we constructed seven formulas with the combination of the selected three lectins, MAL, PHA(L) and EEL (Table 1), using the lectin microarray data of 3 hES cells and 3 differentiated cells (EB) as a training set (Table S1 in Supporting Information). The criterion for classifying undifferentiated and differentiated from of pluripotent cells is as follows: if *Score value* is >0 or equal to 0, cells are categorized into 'pluripotent' cell population, and if *Score value* is <0, cells are categorized into 'nonpluripotent/differentiated' cell population. To evaluate the accuracy of these functions, we used the lectin microarray data of MRC-5-derived iPS cells and MRC-5 parental cells as a test set (Table 2A and Table S2 in Supporting Information). Linear discriminant function with the combination of PHA(L) and EEL (Formula 6: $F = -1.75 \times PHA(L) + 1.28 \times EEL + 1.92$) shows the highest accuracy (100%) of determination of pluripotency, followed by that of MAL and EEL (Formula 5: $F = -2.45 \times MAL + 1.23 \times EEL + 1.45$) (97%), whereas the discriminant function with the combination of three lectins (Formula 7: $F = -2.98 \times MAL + 0.75 \times PHA(L) + 1.44 \times EEL + 0.70$) and MAL and PHA(L) (Formula 4: $F = -2.81 \times MAL + 0.03 \times PHA(L) + 2.29$) shows 86.6% and 55.2%, respectively. Determination with single lectins shows 94.0% (Formula 2: $F = -2.38 \times PHA(L) + 3.46$), 55.2% (Formula 1: $F = -2.78 \times MAL + 2.32$) and 89.6% (Formula 3: $F = 2.59 \times EEL + 1.25$) accuracy. We then analyzed lectin profiles on iPS cells derived from amniotic mesoderm (Nagata *et al.* 2009) (Table 2B, Tables S3 and S5 in Supporting Information). Formula 6 with PHA(L) and EEL as variants generated the highest accuracy (100.0%) among the formulas generated. These results suggest that two lectins, EEL and PHA(L), are most suitable to determine pluripotency of stem cells. To investigate if scores calculated from each formula are correlated with 'pluripotency', we performed RT-PCR analysis of stem cell-specific genes. Positive correlations were observed between the scores and expression of the *OCT4/3* and *NANOG* genes (Fig. 4C).

Table 1 Discriminant functions

No.	Combination of lectins	Formula
1	MAL	$F = -2.78 \times MAL + 2.32$
2	PHA(L)	$F = -2.38 \times PHA(L) + 3.46$
3	EEL	$F = 2.59 \times EEL + 1.25$
4	MAL, PHA(L)	$F = -2.81 \times MAL + 0.03 \times PHA(L) + 2.29$
5	MAL, EEL	$F = -2.45 \times MAL + 1.23 \times EEL + 1.45$
6	PHA(L), EEL	$F = -1.75 \times PHA(L) + 1.28 \times EEL + 1.92$
7	MAL, PHA(L), EEL	$F = -2.98 \times MAL + 0.75 \times PHA(L) + 1.44 \times EEL + 0.70$

Table 2 Evaluation of discriminant functions

Formula number	Sensitivity (%)	Specificity (%)	Accuracy (%)
(A) MRC-derived iPS cells			
1	50	100	55.2
2	93.3	100	94
3	93.3	57.1	89.6
4	50	100	55.2
5	96.7	100	97
6	100	100	100
7	85	100	86.6
(B) AM-derived iPS cells			
1	0	100	16.7
2	10	100	25
3	100	50	91.7
4	0	100	16.7
5	60	100	66.7
6	100	100	100
7	70	100	75

$$\text{Sensitivity} = \frac{\text{Number of true positives}}{\text{Number of true positives} + \text{number of false negatives}}$$

$$\text{Specificity} = \frac{\text{Number of true negatives}}{\text{Number of true negatives} + \text{Number of false positives}}$$

$$\text{Accuracy} = \frac{\text{Number of true positives} + \text{Number of true negatives}}{\text{Number of positives} + \text{Number of negatives}}.$$

Discussion

The goal of this study was to distinguish oligosaccharide structures that are increased in pluripotent and

multipotent cell types. Categorization using lectin probes enabled us to distinguish between different stem cell potencies or to discriminate between undifferentiated and differentiated forms. These results could lead to the use of lectin profiling as a tool for the better understanding of cell identity. To date, global glycan profiles have been preferentially analyzed by mass spectrometry (Satomaa *et al.* 2009; Wollscheid *et al.* 2009). Specifically, high- resolution mass spectrometry is the primary technique for characterizing the structures of individual glycans in most glycomic studies (Satomaa *et al.* 2009; Alvarez-Manilla *et al.* 2010). Mass spectrometry can also be employed to define sites of attachment of glycans to the underlying protein scaffold. A major benefit of mass spectrometry is the detailed information it provides regarding the structure of a glycan. A drawback, however, is its relatively low throughput and the need for different experimental protocols for each glycan subtype. In contrast, lectin microarray can be employed to interrogate the glycome with much higher throughput and provide global information about the types of glycan epitopes that are present in the sample (Kuno *et al.* 2005; Yue & Haab 2009; Porter *et al.* 2010). The high-throughput platform as well as satisfactory sensitivity allows rapid comparison of multiple glycomes in search of global changes that might motivate further mass spectrometry studies.

Glycan-based quality control for cell therapy—Defining the states of pluripotent stem cells

In cell-based therapy, lectin microarray is a practical tool for the quality control of stem cell products. Flow cytometric analysis and immunocytochemical analysis with single probes have been used in this regard, but the lectin microarray technique with multiple probes provides an opportunity to address this issue in a simple, inexpensive and fast manner (Katrlik *et al.* 2010). Cell identity needs to be validated after each step of cell processing, i.e., isolation, *in vitro* propagation, harvesting and transfer because cells may be modified or changed after either of these steps and should thus be monitored by the most trustworthy method. Human ES and iPS cells for potential use as donor cells in cell-based therapy need to be validated for maintenance of the 'undifferentiated' state during *in vitro* propagation and while stored in master and working cell banks (Wobus & Boheler 2005; Yamanaka 2009). Lectin microarray techniques for precise monitoring of the undifferentiated or differentiated state are indeed sensitive and only a small number of cells (1×10^3) are sufficient to obtain reproducible results. This feature of the technology, to define diverse cell identities, also leads to high-throughput screening for drug discovery and toxicology and safety testing.

Glycan profile to determine cell identity

Hematopoietic stem cells were originally defined by GlcNAc-specific wheat germ agglutinin (WGA), one of the most common plant lectins (Spangrude *et al.* 1988), and human and murine endothelial cells were defined by another lectin, α1-2Fuc-specific *Ulex europaeus* agglutinin I (UEA-I) (Jackson *et al.* 1990). Neural stem cells were also defined by the glycolipid antigen LeX/SSEA-1 (Capela & Temple 2002). Furthermore, human ES and iPS cells have been previously evaluated by the presence of carbohydrate markers. The International Stem Cell Initiative characterized 59 human ES cell lines from 17 laboratories worldwide. Human ES cell lines are characterized by carbohydrate markers such as the glycolipid antigens SSEA3 and SSEA4, and the keratan sulfate antigens TRA-1-60, TRA-1-81, GCTM2 and GCT343 as well as the protein antigens (Adewumi *et al.* 2007; Wright & Andrews 2009). In addition to detection of carbohydrate markers by lectins and antibody probes, comprehensive glycan analysis serves as another method to detect and define cell identities. In this study, we found the pluripotent stem cells have the specific glycan structure, Galα1-3Gal, recognized by EEL (Fig. S1 in Supporting Information). Their major specific N-glycosylation feature in hES cells is complex fucosylation (Satomaa *et al.* 2009), whereas PHA(E) ligands are signs of hES cell differentiation (Venable *et al.* 2005; Wearne *et al.* 2006). This study suggests that glycan profiling by lectin microarray is more sensitive, compared with any other analysis. Further analysis of stem cell glycan may also lead to establishing new glycan structures as stem cell markers in addition to the commonly used SSEA and TRA glycan structures.

Glycans function as ligands for specific glycan receptors and modulate the activity of their carrier proteins and lipids (Imperiali & O'Connor 1999; Zanetta & Vergoten 2003). More than half of all proteins in a human cell are glycosylated. Consequently, a global change in protein-linked glycan biosynthesis can simultaneously modulate the properties of multiple proteins. It is likely that drastic changes during differentiation of human stem cells have major influences on a number of cellular signaling cascades and affect biological processes within the cells (Xu *et al.* 2005; Sasaki *et al.*

2008). Thus, glycan profiling can be useful for validation of cell identity (Satomaa *et al.* 2009). Categorization of stem cells by lectin microarray analysis can become another fundamental method in addition to immunocytochemistry and flow cytometric analysis. Microarray technologies currently enhance our understanding of gene expression, genomic stability and epigenetics, are commonly used in research laboratories and clinics today, and will likely play important roles in advancing stem cell research. In the future, analysis of stem cell glycan structure may be useful for establishing new markers beyond the lectin markers that already play a major role in the rapidly evolving world of stem cell biology.

Experimental procedures

Cells and cell culture

9-15c (uncommitted stem cells), H-1/A (preadipocytes), KUM5 (chondroblasts) and KUSA-A1 (osteoblasts) are available through cell banks (JHSF cell bank: http://www.jhsf.or.jp/English/index_gc.html; RIKEN cell bank: http://www.brc.riken.go.jp/lab/cell/english/). 9-15c (Yamada *et al.* 2007), H-1/A (Umezawa *et al.* 1991), KUM5 (Sugiki *et al.* 2007) and KUSA-A1 cells (Umezawa *et al.* 1992) were cultured using methods described previously. The cells were maintained in POWEREDBY10 medium (MED SHIROTORI CO., Ltd, Tokyo, Japan) or Iscove's modified Dulbecco's medium (IMDM) supplemented with 20% fetal bovine serum and penicillin (100 μg/mL)/streptomycin (100 μg/mL)/amphotericin B (250 ng/mL) at 33 °C with 5% CO_2. Human mesenchymal cells were maintained in DMEM (Sigma, St. Louis, MO) supplemented with 100 μg/mL penicillin, 100 IU/mL streptomycin and 10% fetal calf serum at 37 °C in a CO_2 incubator. Human embryonal carcinoma cell line NCR-G3, from a testicular tumor, was cultured in G031101 medium (Med Shirotori, Tokyo, Japan) as previously described (Maruyama *et al.* 1996; Umezawa *et al.* 1996). Human iPS cells were cultured in Valuegen medium (Med Shirotori, Tokyo, Japan) (Makino *et al.* 2009; Nagata *et al.* 2009).

Extraction of membrane fractions and lectin microarray analysis

Cells ($0.1–1 \times 10^6$) were washed with PBS and collected with a cell scraper. Cell pellets of hES-3, -8, and -9 cells (Osafune *et al.* 2008) were kindly obtained from Dr Douglas Melton (Harvard University). Cell membrane fractions were extracted from the cell pellets using a CelLytic MEM Protein Extraction kit (Sigma, St Louis, MO, USA). Lectin microarray analysis was performed as previously described (Kuno *et al.* 2005, 2008). Briefly, a small aliquot of protein fraction (200 ng) was labeled with Cy3-succinimidyl ester (designated as Cy3-labeled glycoprotein). The lectin chip with 43 lectins (Kuno *et al.* 2005) for mouse cells or LecChip™ with 45 lectins (GP Bio-Sciences, Kanagawa, Japan) for human cells was incubated with the Cy3-labeled glycoprotein solution (100 μL) at a concentration of 0.25 and 0.5 μg/mL in probing buffer (TBS containing 0.05% Triton X-100) at 4 °C until binding reached equilibrium. Lectins are well known as glycan recognizers and are classified into several categories, for instance, fucose, sialic acid, asialo-form, agalacto-form, high mannose, O-glycan and branching structure recognizers (Fig. S1 in Supporting Information). We calculated the net intensity value for each spot by subtracting a background value from signal intensity and then averaged the signal net intensity values of three spots. Lectin microarray data on each cell type were processed by the microarray system using a max-normalization procedure after a gain-merging process (Kuno *et al.* 2008).

Hierarchical clustering analysis and principal component analysis

To analyze the lectin microarray data, we used agglomerative hierarchical clustering and principal component analysis (PCA) (Sharov *et al.* 2005). The hierarchical clustering techniques classify data by similarity and their results are represented by dendrograms. PCA is a multivariate analysis technique that finds major patterns in data variability.

Discriminant analysis of pluripotency in human pluripotent stem cells

Coefficients and constants of each formula were defined, using the lda function in the MASS library of the statistical package R [http://www.r-project.org/, (Venables & Ripley 2002), (Ripley 1996)].

Acknowledgement

We express our sincere thanks to C. Ketcham for reviewing the manuscript, M. Yamada for fruitful discussion and critical reading of the manuscript, Y. Takahashi for providing expert technical assistance and to K. Saito and Y. Kajiyama for secretarial work. This work was supported in part by a grant for New Energy and Industrial Technology Development Organization (NEDO) in Japan; Health and Labour Sciences Research Grants; and grants from the Ministry of Education, Culture, Sports, Science and Technology (MEXT) of Japan.

References

Adewumi, O., Aflatoonian, B., Ahrlund-Richter, L., *et al.* (2007) Characterization of human embryonic stem cell lines by the international stem cell initiative. *Nat. Biotechnol.* **25**, 803–816.

Alvarez-Manilla, G., Warren, N.L., Atwood, J. III, Orlando, R., Dalton, S. & Pierce, M. (2010) Glycoproteomic analysis of embryonic stem cells: identification of potential glycobiomarkers using lectin affinity chromatography of glycopeptides. *J. Proteome Res.* **9**, 2062–2075.

Angeloni, S., Ridet, J.L., Kusy, N., Gao, H., Crevoisier, F., Guinchard, S., Kochhar, S., Sigrist, H. & Sprenger, N. (2005) Glycoprofiling with micro-arrays of glycoconjugates and lectins. *Glycobiology* **15**, 31–41.

Aoi, T., Yae, K., Nakagawa, M., Ichisaka, T., Okita, K., Takahashi, K., Chiba, T. & Yamanaka, S. (2008) Generation of pluripotent stem cells from adult mouse liver and stomach cells. *Science* **321**, 699–702.

Budnik, B.A., Lee, R.S. & Steen, J.A. (2006) Global methods for protein glycosylation analysis by mass spectrometry. *Biochim. Biophys. Acta* **1764**, 1870–1880.

Capela, A. & Temple, S. (2002) LeX/ssea-1 is expressed by adult mouse CNS stem cells, identifying them as nonependymal. *Neuron* **35**, 865–875.

Ebe, Y., Kuno, A., Uchiyama, N., Koseki-Kuno, S., Yamada, M., Sato, T., Narimatsu, H. & Hirabayashi, J. (2006) Application of lectin microarray to crude samples: differential glycan profiling of lec mutants. *J. Biochem.* **139**, 323–327.

Imperiali, B. & O'Connor, S.E. (1999) Effect of N-linked glycosylation on glycopeptide and glycoprotein structure. *Curr. Opin. Chem. Biol.* **3**, 643–649.

Jackson, C.J., Garbett, P.K., Nissen, B. & Schrieber, L. (1990) Binding of human endothelium to Ulex europaeus I-coated Dynabeads: application to the isolation of microvascular endothelium. *J. Cell Sci.* **96** (Pt 2), 257–262.

Kaichi, S., Hasegawa, K., Takaya, T., Yokoo, N., Mima, T., Kawamura, T., Morimoto, T., Ono, K., Baba, S., Doi, H., Yamanaka, S., Nakahata, T. & Heike, T. (2010) Cell line-dependent differentiation of induced pluripotent stem cells into cardiomyocytes in mice. *Cardiovasc. Res.* **88**, 314–323.

Katrlik, J., Svitel, J., Gemeiner, P., Kozar, T. & Tkac, J. (2010) Glycan and lectin microarrays for glycomics and medicinal applications. *Med. Res. Rev.* **30**, 394–418.

Kuno, A., Itakura, Y., Toyoda, M., Takahashi, Y., Yamada, Y., Umezawa, A. & Hirabayashi, J. (2008) Development of a data-mining system for differential profiling of cell glycoproteins based on lectin microarray. *J. Proteomics Bioinform.* **1**, 068–072.

Kuno, A., Uchiyama, N., Koseki-Kuno, S., Ebe, Y., Takashima, S., Yamada, M. & Hirabayashi, J. (2005) Evanescent-field fluorescence-assisted lectin microarray: a new strategy for glycan profiling. *Nat. Methods* **2**, 851–856.

Lee, J.H., Schell, M.J. & Roetzheim, R. (2009) Analysis of group randomized trials with multiple binary endpoints and small number of groups. *PLoS ONE* **4**, e7265.

Makino, H., Toyoda, M., Matsumoto, K., *et al.* (2009) Mesenchymal to embryonic incomplete transition of human cells by chimeric OCT4/3 (POU5F1) with physiological co-activator EWS. *Exp. Cell Res.* **315**, 2727–2740.

Maruyama, T., Umezawa, A., Kusakari, S., Kikuchi, H., Nozaki, M. & Hata, J. (1996) Heat shock induces differentiation of human embryonal carcinoma cells into trophectoderm lineages. *Exp. Cell Res.* **224**, 123–127.

Matsumoto, S., Shibuya, I., Kusakari, S., Segawa, K., Uyama, T., Shimada, A. & Umezawa, A. (2005) Membranous osteogenesis system modeled with KUSA-A1 mature osteoblasts. *Biochim. Biophys. Acta* **1725**, 57–63.

Nagata, S., Toyoda, M., Yamaguchi, S., Hirano, K., Makino, H., Nishino, K., Miyagawa, Y., Okita, H., Kiyokawa, N., Nakagawa, M., Yamanaka, S., Akutsu, H., Umezawa, A. & Tada, T. (2009) Efficient reprogramming of human and mouse primary extra-embryonic cells to pluripotent stem cells. *Genes Cells* **14**, 1395–1404.

Osafune, K., Caron, L., Borowiak, M., Martinez, R.J., Fitz-Gerald, C.S., Sato, Y., Cowan, C.A., Chien, K.R. & Melton, D.A. (2008) Marked differences in differentiation propensity among human embryonic stem cell lines. *Nat. Biotechnol.* **26**, 313–315.

Pilobello, K.T., Krishnamoorthy, L., Slawek, D. & Mahal, L.K. (2005) Development of a lectin microarray for the rapid analysis of protein glycopatterns. *Chembiochem* **6**, 985–989.

Porter, A., Yue, T., Heeringa, L., Day, S., Suh, E. & Haab, B.B. (2010) A motif-based analysis of glycan array data to determine the specificities of glycan-binding proteins. *Glycobiology* **20**, 369–380.

Ripley, B.D. (1996) *Pattern Recognition and Neural Networks.* Cambridge: Cambridge University Press.

Sasaki, N., Okishio, K., Ui-Tei, K., Saigo, K., Kinoshita-Toyoda, A., Toyoda, H., Nishimura, T., Suda, Y., Hayasaka, M., Hanaoka, K., Hitoshi, S., Ikenaka, K. & Nishihara, S. (2008) Heparan sulfate regulates self-renewal and pluripotency of embryonic stem cells. *J. Biol. Chem.* **283**, 3594–3606.

Satomaa, T., Heiskanen, A., Mikkola, M., *et al.* (2009) The N-glycome of human embryonic stem cells. *BMC Cell Biol.* **10**, 42.

Sharon, N. & Lis, H. (2004) History of lectins: from hemagglutinins to biological recognition molecules. *Glycobiology* **14**, 53R–62R.

Sharov, A.A., Dudekula, D.B. & Ko, M.S. (2005) A web-based tool for principal component and significance analysis of microarray data. *Bioinformatics (Oxford, England)* **21**, 2548–2549.

Spangrude, G.J., Heimfeld, S. & Weissman, I.L. (1988) Purification and characterization of mouse hematopoietic stem cells. *Science* **241**, 58–62.

Sugiki, T., Uyama, T., Toyoda, M., Morioka, H., Kume, S., Miyado, K., Matsumoto, K., Saito, H., Tsumaki, N., Takahashi, Y., Toyama, Y. & Umezawa, A. (2007) Hyaline cartilage formation and enchondral ossification modeled with KUM5 and OP9 chondroblasts. *J. Cell. Biochem.* **100**, 1240–1254.

Takahashi, K., Tanabe, K., Ohnuki, M., Narita, M., Ichisaka, T., Tomoda, K. & Yamanaka, S. (2007) Induction of pluripotent stem cells from adult human fibroblasts by defined factors. *Cell* **131**, 861–872.

Tateno, H., Uchiyama, N., Kuno, A., Togayachi, A., Sato, T., Narimatsu, H. & Hirabayashi, J. (2007) A novel strategy for mammalian cell surface glycome profiling using lectin microarray. *Glycobiology* **17**, 1138–1146.

Umezawa, A., Maruyama, T., Inazawa, J., Imai, S., Takano, T. & Hata, J. (1996) Induction of mcl1/EAT, Bcl-2 related gene, by retinoic acid or heat shock in the human embryonal carcinoma cells, NCR-G3. *Cell Struct. Funct.* **21**, 143–150.

Umezawa, A., Maruyama, T., Segawa, K., Shadduck, R.K., Waheed, A. & Hata, J. (1992) Multipotent marrow stromal cell line is able to induce hematopoiesis *in vivo*. *J. Cell. Physiol.* **151**, 197–205.

Umezawa, A., Tachibana, K., Harigaya, K., Kusakari, S., Kato, S., Watanabe, Y. & Takano, T. (1991) Colony-stimulating factor 1 expression is down-regulated during the adipocyte differentiation of H-1/A marrow stromal cells and induced by cachectin/tumor necrosis factor. *Mol. Cell. Biol.* **11**, 920–927.

Varki, A. (1993) Biological roles of oligosaccharides: all of the theories are correct. *Glycobiology* **3**, 97–130.

Venable, A., Mitalipova, M., Lyons, I., Jones, K., Shin, S., Pierce, M. & Stice, S. (2005) Lectin binding profiles of SSEA-4 enriched, pluripotent human embryonic stem cell surfaces. *BMC Dev. Biol.* **5**, 15.

Venables, W.N. & Ripley, B.D. (2002) *Modern Applied Statistics with S*, 4th edn. New York: Springer.

Wearne, K.A., Winter, H.C., O'Shea, K. & Goldstein, I.J. (2006) Use of lectins for probing differentiated human embryonic stem cells for carbohydrates. *Glycobiology* **16**, 981–990.

Wobus, A.M. & Boheler, K.R. (2005) Embryonic stem cells: prospects for developmental biology and cell therapy. *Physiol. Rev.* **85**, 635–678.

Wollscheid, B., Bausch-Fluck, D., Henderson, C., O'Brien, R., Bibel, M., Schiess, R., Aebersold, R. & Watts, J.D. (2009) Mass-spectrometric identification and relative quantification of N-linked cell surface glycoproteins. *Nat. Biotechnol.* **27**, 378–386.

Wright, A.J. & Andrews, P.W. (2009) Surface marker antigens in the characterization of human embryonic stem cells. *Stem Cell Res.* **3**, 3–11.

Xu, R.H., Peck, R.M., Li, D.S., Feng, X., Ludwig, T. & Thomson, J.A. (2005) Basic FGF and suppression of BMP signaling sustain undifferentiated proliferation of human ES cells. *Nat. Methods* **2**, 185–190.

Yamada, Y., Sakurada, K., Takeda, Y., Gojo, S. & Umezawa, A. (2007) Single-cell-derived mesenchymal stem cells overexpressing Csx/Nkx2.5 and GATA4 undergo the stochastic cardiomyogenic fate and behave like transient amplifying cells. *Exp. Cell Res.* **313**, 698–706.

Yamanaka, S. (2009) A fresh look at iPS cells. *Cell* **137**, 13–17.

Yu, J., Vodyanik, M.A., Smuga-Otto, K., Antosiewicz-Bourget, J., Frane, J.L., Tian, S., Nie, J., Jonsdottir, G.A., Ruotti, V., Stewart, R., Slukvin, I.I. & Thomson, J.A. (2007) Induced pluripotent stem cell lines derived from human somatic cells. *Science* **318**, 1917–1920.

Yue, T. & Haab, B.B. (2009) Microarrays in glycoproteomics research. *Clin. Lab. Med.* **29**, 15–29.

Zanetta, J.P. & Vergoten, G. (2003) Lectin domains on cytokines. *Adv. Exp. Med. Biol.* **535**, 107–124.

Received: 3 August 2010
Accepted: 19 September 2010

Supporting Information/Supplementary material

The following Supporting Information can be found in the online version of the article:

Figure S1 List of lectins on LecChip™ and their specificity.

Figure S2 Signal intensities of each lectin on LecChip™.

Table S1 Scores of ES and EB cells by each formula

Table S2 Scores of iPS cells and their parental cells (MRC-5) by each formula

Table S3 Scores of iPS cells and their parental cells (AM936EP) by each formula

Table S4 Cell name of MRC-derived iPS cells

Table S5 Cell name of AM-derived iPS cells

Additional Supporting Information may be found in the online version of this article.

Please note: Wiley-Blackwell are not responsible for the content or functionality of any supporting materials supplied by the authors. Any queries (other than missing material) should be directed to the corresponding author for the article.

OPEN ACCESS Freely available online

PLoS one

Defining Hypo-Methylated Regions of Stem Cell-Specific Promoters in Human iPS Cells Derived from Extra-Embryonic Amnions and Lung Fibroblasts

Koichiro Nishino[1], Masashi Toyoda[1], Mayu Yamazaki-Inoue[1], Hatsune Makino[1], Yoshihiro Fukawatase[1], Emi Chikazawa[1], Yoriko Takahashi[1], Yoshitaka Miyagawa[2], Hajime Okita[2], Nobutaka Kiyokawa[2], Hidenori Akutsu[1], Akihiro Umezawa[1]*

1 Department of Reproductive Biology, National Institute for Child Health and Development, Tokyo, Japan, **2** Department of Developmental Biology, National Institute for Child Health and Development, Tokyo, Japan

Abstract

Background: Human induced pluripotent stem (iPS) cells are currently used as powerful resources in regenerative medicine. During very early developmental stages, DNA methylation decreases to an overall low level at the blastocyst stage, from which embryonic stem cells are derived.Therefore, pluripotent stem cells, such as ES and iPS cells, are considered to have hypo-methylated status compared to differentiated cells. However, epigenetic mechanisms of "stemness" remain unknown in iPS cells derived from extra-embryonic and embryonic cells.

Methodology/Principal Findings: We examined genome-wide DNA methylation (24,949 CpG sites covering 1,3862 genes, mostly selected from promoter regions) with six human iPS cell lines derived from human amniotic cells and fetal lung fibroblasts as well as two human ES cell lines, and eight human differentiated cell lines using Illumina's Infinium HumanMethylation27. A considerable fraction (807 sites) exhibited a distinct difference in the methylation level between the iPS/ES cells and differentiated cells, with 87.6% hyper-methylation seen in iPS/ES cells. However, a limited fraction of CpG sites with hypo-methylation was found in promoters of genes encoding transcription factors. Thus, a group of genes becomes active through a decrease of methylation in their promoters. Twenty-three genes including *SOX15*, *SALL4*, *TDGF1*, *PPP1R16B* and *SOX10* as well as *POU5F1* were defined as genes with hypo-methylated SS-DMR (Stem cell-Specific Differentially Methylated Region) and highly expression in iPS/ES cells.

Conclusions/Significance: We show that DNA methylation profile of human amniotic iPS cells as well as fibroblast iPS cells, and defined the SS-DMRs. Knowledge of epigenetic information across iPS cells derived from different cell types can be used as a signature for "stemness" and may allow us to screen for optimum iPS/ES cells and to validate and monitor iPS/ES cell derivatives for human therapeutic applications.

Citation: Nishino K, Toyoda M, Yamazaki-Inoue M, Makino H, Fukawatase Y, et al. (2010) Defining Hypo-Methylated Regions of Stem Cell-Specific Promoters in Human iPS Cells Derived from Extra-Embryonic Amnions and Lung Fibroblasts. PLoS ONE 5(9): e13017. doi:10.1371/journal.pone.0013017

Editor: Tadafumi Kato, RIKEN Brain Science Institution, Japan

Received April 21, 2010; **Accepted** September 6, 2010; **Published** September 27, 2010

Funding: This study was supported by grants from the Ministry of Education, Culture, Sports, Science, and Technology (MEXT) of Japan; Ministry of Health, Labour and Welfare Sciences (MHLW) research grants; by a Research Grant on Health Science focusing on Drug Innovation from the Japan Health Science Foundation; by the program for the promotion of Fundamental Studies in Health Science of the Pharmaceuticals and Medical Devices Agency; by a Research Grant for Cardiovascular Disease from the MHLW; and by a Grant for Child Health and Development from the MHLW. The funders had no role in study design, data collection and analysis, decision to publish, or preparation of the manuscript.

Competing Interests: The authors have declared that no competing interests exist.

* E-mail: umezawa@1985.jukuin.keio.ac.jp

Introduction

Human embryonic stem (ES) cells [1] and induced pluripotent stem (iPS) cells [2,3,4,5] are currently used as powerful resources in regenerative medicine. However, epigenetic mechanisms of "stemness" remain unknown. DNA methylation is known to be a key component in normal differentiation and development [6,7]. Tissue-specific genes, such as *OCT-4/3* [8], *Sry* (sex determining region on Y chromosome) [9] and *MyoD* [10], show tissue-specific demethylation corresponding to their expression during development. Furthermore, DNA methylation in cells specifically varies depending on cell lineage and tissue types [7]. Transformation to iPS cells from differentiated cells requires a process of epigenetic reprogramming [11]. Understanding the epigenetic regulation in human pluripotent stem cells, therefore, enable us to elucidate "stemness" and to screen for optimum iPS/ES cells for human therapeutic applications. Human extra-embryonic amnion cells are a useful cell source for generation of iPS cells, because they can be collected without invasion and are conventionally freeze-storable. Recently, we generated iPS cells from human amnion cells as well as human fetal lung fibroblast cells [12,13]. Here, we show DNA methylation profiles of human pluripotent stem cells including iPS cells, which were derived from extra-embryonic amnion cells and fetal lung fibroblast cells, and human ES cells. We also defined another subset that may play a key practical role in maintaining the state of "stemness".

Results

Analysis of genome-wide DNA methylation

Human iPS cell lines (MRC-iPS [13] and AM-iPS cell lines [12]) independently established in our laboratory by retroviral infection of 4 genes (*OCT-3/4*, *SOX2*, *c-MYC*, and *KLF4*), based on the Yamanaka's pioneer protocols [2] from 2 fully differentiated cells (MRC-5, fetal lung fibroblast cells, and AM936EP, amnion cells), were used as a primary source for experimentation (Table 1). These cells clearly showed human iPS characters [12,13].

To examine DNA methylation status in six iPS, two ES [14], and eight differentiated cell lines (Table 1), we therefore examined genome-wide DNA methylation using Illumina's Infinium HumanMethylation27 BeadChip, on which oligonucleotides for 27,578 CpG sites covering more than 14,000 genes are mounted, mostly selected from promoter regions. This assay system provides advantageous quantitative measurement. DNA methylation levels were recorded using a scoring system ranging from "0" (completely unmethylated) to "1" (fully-methylated). Using multiple repetitions, we analyzed 24,949 out of 27,578 CpG sites with 16 samples (see Materials and Methods), categorizing them into three groups; Low (score≤0.3), Middle (0.3<score≤0.7), or High (0.7<score) methylation. Overall, methylation levels in pluripotent stem cells and differentiated cells are shown in Fig. 1A, with the levels in each cell line presented in Table S1. While the percentage of the High class in differentiated cells was 16.3% on average, the percentage in iPS/ES cells was 25.3% (Fig. 1A). The number of CpG sites categorized in the High class is significantly greater in pluripotent stem cells compared with differentiated cells. Hierarchical clustering analysis clearly discriminates iPS/ES cells from the differentiated cells (Fig. 1B). Hyper-methylated sites (shown in red) are widespread in the heat map in iPS/ES cells, compared with the differentiated cells (Fig. 1B), suggesting that gene promoters in iPS/ES cells are hyper-methylated, compared with those in differentiated cells.

About two-thirds of the CpG sites were at a Low methylated level in both iPS/ES cell and differentiated cell groups (Fig. 1A and B). Another computation found 13,971 CpG sites to consistently show a score of lower than 0.3. This suggests that a significant fraction of the CpG sites examined may have less involvement in methylation, although some might become methylated under different conditions. As most CpG sites on the chip were chosen simply based on the location in promoters, it is possible that some CpG sites may be positioned at a distance from the target site, even in a promoter controlled by DNA methylation. Analysis of our and all published data indicated that a group of CpG sites more suitable to methylation analyses could be identified, allowing us to focus attention on specific changes in methylation levels seen between iPS/ES and differentiated cells.

Differentially methylated site (DMS) in the promoters. Firstly, we defined the "differentially methylated site" (DMS), representing a CpG site whose score differed 0.3 points and more between the two cell groups. The DMSs between MRC-iPS and AM-iPS cells, and also between iPS and ES cells, were only 1.0% and 2.8% of all the CpG sites, respectively (Fig. 1C), suggesting that iPS and ES cells have similar methylation status. In contrast, the DMSs between AM936EP and AM-iPS cells, and between MRC-5 and MRC-iPS cells, were 11.3% and 10.6%, respectively, suggesting that iPS cells and their parental cells have differentially methylated status (Fig. 1C and D). It should be noted that approximately 80% of the DMSs between the iPS cells and their parental cells changed to a "hyper-methylated" state from a "hypo-methylated" state in iPS cells (Fig. 1C). Comparison of DMSs between AM- and MRC-iPS cells, and between iPS and ES cells show slight but significant difference (Fig. 1C). In 261 DMSs between MRC- and AM-iPS cells (MA-DMSs), 203 sites in AM-iPS cells and 165 in MRC-iPS cells showed no difference from their parental cells, suggesting that these sites in iPS cells are inherited from their tissue origin (Fig. 1E). In addition, 414 out of 694 DMSs between MRC-iPS and ES cells (ME-DMSs) and 581 out of 990 DMSs between AM-iPS and ES cells (AE-DMSs) are inherited DMSs (Fig. 1E). Interestingly, approximately 40% of DMSs between iPS and ES cells are iPS-specific DMSs, meaning that these sites are aberrant methylated in iPS cells (Fig. 1E). In

Table 1. A list of human cells analyzed for a methylation state in this study.

Cell ID	Description	ability of differentiation
MRC5	Fetal lung fibroblast cells	None
MRC-iPS-11	MRC5-derived iPS cells (P4)	Pluripotent
MRC-iPS-19	MRC5-derived iPS cells (P4)	Pluripotent
MRC-iPS-75	MRC5-derived iPS cells (P4)	Pluripotent
AM936EP	Amnion-derived cells (P6)	None
AM-iPS-3	AM936EP -derived iPS cells (P4)	Pluripotent
AM-iPS-6	AM936EP -derived iPS cells (P4)	Pluripotent
AM-iPS-8	AM936EP -derived iPS cells (P4)	Pluripotent
UtE1104	Endometrium-derived cells (P7)	None
H4-1	Bone marrow stroma-derived cells (P26)	None
Mim1508E	Auricular cartilage-derived cells (P1)	Cartilage
Yub636BM	Extra finger bone marrow-derived cells (P3)	Bone
PAE551	Placental artery endothelial cells (P13)	None
Edom22	Menstrual blood-derived cells (P1)	Myoblast
HUES3	Embryonic stem cells (P29)	Pluripotent
HUES8	Embryonic stem cells (P24)	Pluripotent

Numbers in parenthesis with P indicate passage in culture on the cells used in the methylation analysis.
doi:10.1371/journal.pone.0013017.t001

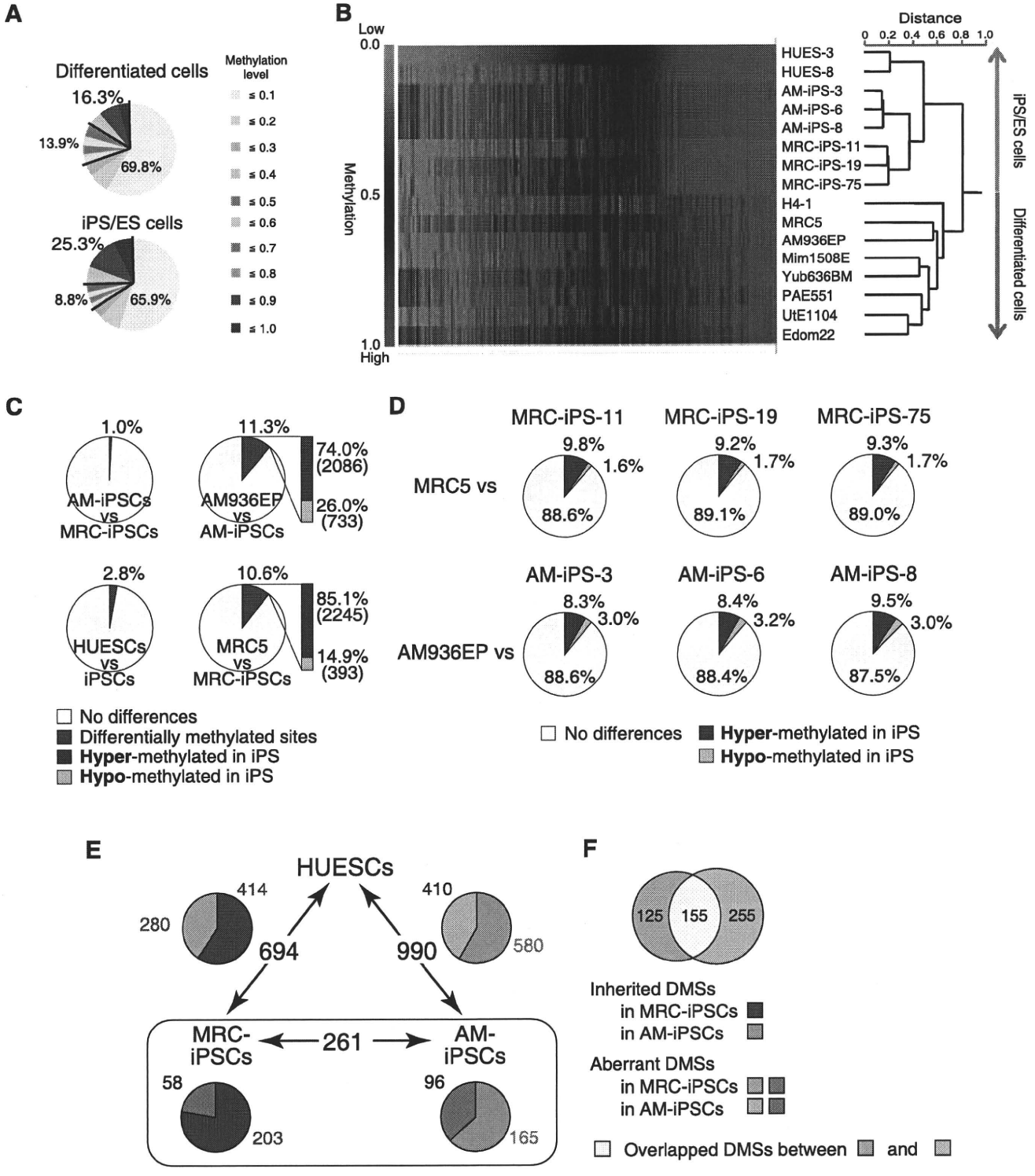

Figure 1. The ratio of hyper-methylated sites in iPS/ES cells was significantly larger than that of the differentiated cells. (**A**) Ratio of Low (methylation score≤0.3), Middle (0.3<score≤0.7), and High (0.7<score) methylated states in 24,949 CpG sites. (**B**) Clustering analysis. Heat map showing hyper-methylation in human iPS/ES cells compared with differentiated cells. The Heat map in hierarchical clustering analysis represented DNA methylation levels from completely methylated (red) to unmethylated (green). Epigenetic distances (Euclidean Distance) were calculated by NIA Array. (**C**) Comparisons of CpG sites between two groups show high similarities between AM-iPS and MRC-iPS cells or between human ES cells (HUESCs) and iPS cells (iPSCs). In contrast, 11.3% and 10.6% of CpG sites are differentially methylated in AM-iPS and MRC-iPS cells, respectively, compared to their parental cells (AM936EP and MRC5). It should be noted that 74.0% and 85.1% of the differentially methylated sites (DMSs) are hyper-methylated in AM-iPS and MRC-iPS cells, respectively, compared to their parental cells. (**D**) Comparison of the 24,949 CpG sites between iPS cells and their parental cells. (**E**) DMSs among human ES cells, AM- and MRC-iPS cells. The relative amount of inherited/aberrant DMSs is indicated in the pie chart. (**F**) Overlapped aberrant DMSs between MRC- and AM-iPS cells.
doi:10.1371/journal.pone.0013017.g001